Supplemental Information

Images Preprocessing & Analyses

Details of GBCr processing and analysis methods were previously described (1-10). Briefly, the preprocessing of each *f*MRI included brain extraction, motion correction, slice-time correction, spatial smoothing (FWHM 5 mm), high-pass temporal filtering (100 s), nonlinear registration of structural images to a standard Montreal Neurological Institute (MNI) template (2x2x2 mm), boundary-based registration (BBR) of *f*MRI to high-resolution images, and regression of motion parameters, cerebrospinal fluid (CSF), white matter, and global brain signal, and their 1st derivatives. In addition, motion scrubbing, as per Power et al. (11), was completed prior to GBCr calculation. We have used GBCr, instead of GBC without global signal regression (GBCnr), because of the study hypotheses were based on previous GBCr findings (1-5, 7, 12), which provided the rationale for the current report and will facilitate the interpretation of the study findings. Of notes, in previous studies we found no GBCnr alteration in TRD and ketamine had no effects on GBCnr levels (1).

Time series were extracted from all voxels within each individual's anatomically defined whole-brain GM mask. Matrices of pairwise Pearson correlation coefficients of all GM voxels were generated, and then transformed to Fisher z values. For each voxel, GBCr is calculated as the normalized average across those Fisher z values, which generates a map for each subject where each voxel value represents the functional connectivity strength of that voxel with the rest of the brain. In graph theory terms, GBCr (also known as Functional Connectivity Strength; FCS (12)) is considered a measure of nodal strength of a voxel in the whole brain network – determining brain hubs and examining the coherence between a local region and the rest of the brain (13). All processing and analyses were conducted in the subject functional space, except for 2nd level group analyses (MNI space; 2x2x2 mm). All included scans passed the following quality control criteria: no BOLD run with a single frame movement greater than 1 functional voxel and no motion scrubbing of more than 50% of each run. Absolute motion, relative motion, and scrubbing did not differ between TRD and HC in Cohort A, and between sessions in Cohort B (all p values > 0.05).

The publically available software package Freesurfer (http://surfer.nmr.mgh.harvard.edu) was used for MRI image processing and segmentation, as previously described (14-16). Each PFC mask included the following right and left regions: caudal anterior cingulate, caudal middle frontal, lateral orbitofrontal, medial orbitofrontal, pars opercularis, pars orbitalis, pars triangularis, rostral anterior cingulate, rostral middle frontal, superior frontal, and frontal pole. The vPFC included the limbic component of the PFC in the connectivity-based atlas of 7 brain connectivity networks by Yeo et al. (17) (see Figure 4A).

To address any potential effects by the oddball task, Cohort B assessments used a balanced design; i.e. we only investigated the connectivity differences between *f*MRI runs all of which include the visual oddball task. Nonetheless, previous studies have shown highly overlapping architecture of connectivity during rest and various task *f*MRI (18). In a methodology study using GBCr as outcome and including resting-state as well as 7 various

task *f*MRI, Cole and colleagues found similar results with and without task activation regressions (19).

Statistical Analyses

The distribution of outcome measures was examined using probability plots and test statistics. Transformations and non-parametric tests were used as necessary. Estimates of variation are provided as standard error of the mean (SEM). Voxel-wise *f*MRI analyses used FSL Randomise with 5000 permutations and cluster-based thresholding ($z > 1.96$, corrected $\alpha = 0.05$) (20). We have limited our investigation to the PFC, 1st because of its critical role in depression, 2nd because previous findings of reduced GBCr were limited to the PFC, and 3rd to limit Type I & Type II errors and facilitate the interpretation of the findings.

Voxel-wise PFC GBCr were compared between TRD and matched HC using independent *t*-test. Average GBCr in the clusters that showed significantly lower GBCr in the TRD were extracted at baseline and 24h post ketamine treatment. Paired *t*-test was used to examine the effects of ketamine and placebo on the average GBCr in these clusters. The results of paired *t*-test in these small samples were confirmed using Related-Samples Wilcoxon Signed Rank Test and bootstrapping of effect size (mean divided by standard deviation) with 10,000 iterations. To illustrate the behavioral effects of treatment in TRD subjects, a repeated measure general linear model (GLM) examined the effects of treatment (placebo vs. ketamine), time (baseline vs. 24h), and treatment-by-time interaction. To explore whether baseline GBCr predicted improvement, we constructed a GLM examining the GBCr-by-treatment interaction and GBCr effects on percent improvement in depression severity.

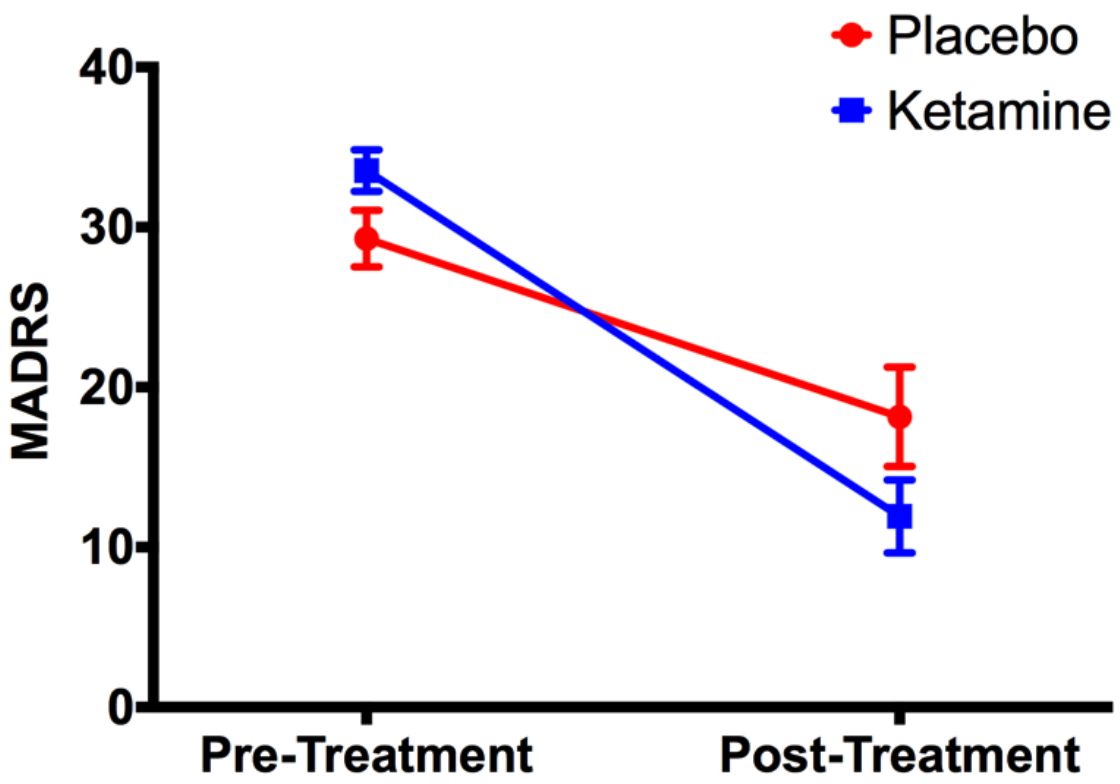

Figure S1. Treatment effects on depression severity. *Abbreviations*: MADRS = Montgomery-Åsberg Depression Rating Scale.

Table S1. Significant GBCr clusters.

Region	Side	Coordinates (Peak)	Size (mm^3)	Effects
TRD vs. HC (Figure 1)				
Dorsomedial	R	8,24, 36	1316	TRD < HC
Dorsolateral	R	20,26,46	854	TRD < HC
Dorsomedial	L	-6,8,58	854	TRD < HC
Lamotrigine Effects (Figure 2A)				
Medial	L R	-12,18,44	1634	Plc > Lamo
Ketamine Effects (Figure 2B)				
Dorsomedial	L R	-12,8,62	1726	Plc < Ket
Frontolateral	L	-56,6,32	1524	Plc < Ket

Notes: The name of the region point to the location of the cluster in the figures. The anatomical locations are depicted in the figures. *Abbreviations* – GBCr: global brain connectivity with global signal regression; TRD: treatment-resistant depression; HC: healthy control; Plc: placebo; Lamo: lamotrigine; Ket: ketamine; L: left; R: right.

References:

1. Abdallah CG, Averill LA, Collins KA, Geha P, Schwartz J, Averill C, et al. (2016): Ketamine Treatment and Global Brain Connectivity in Major Depression. *Neuropsychopharmacology*.
2. Murrough JW, Abdallah CG, Anticevic A, Collins KA, Geha P, Averill LA, et al. (2016): Reduced global functional connectivity of the medial prefrontal cortex in major depressive disorder. *Hum Brain Mapp*.
3. Anticevic A, Brumbaugh MS, Winkler AM, Lombardo LE, Barrett J, Corlett PR, et al. (2013): Global prefrontal and fronto-amygdala dysconnectivity in bipolar I disorder with psychosis history. *Biol Psychiatry*. 73:565-573.
4. Anticevic A, Corlett PR, Cole MW, Savic A, Gancsos M, Tang Y, et al. (2015): N-methyl-D-aspartate receptor antagonist effects on prefrontal cortical connectivity better model early than chronic schizophrenia. *Biol Psychiatry*. 77:569-580.
5. Anticevic A, Hu S, Zhang S, Savic A, Billingslea E, Wasylink S, et al. (2014): Global resting-state functional magnetic resonance imaging analysis identifies frontal cortex, striatal, and cerebellar dysconnectivity in obsessive-compulsive disorder. *Biol Psychiatry*. 75:595-605.
6. Anticevic A, Hu X, Xiao Y, Hu J, Li F, Bi F, et al. (2015): Early-course unmedicated schizophrenia patients exhibit elevated prefrontal connectivity associated with longitudinal change. *J Neurosci*. 35:267-286.
7. Cole MW, Anticevic A, Repovs G, Barch D (2011): Variable global dysconnectivity and individual differences in schizophrenia. *Biol Psychiatry*. 70:43-50.
8. Cole MW, Yarkoni T, Repovs G, Anticevic A, Braver TS (2012): Global connectivity of prefrontal cortex predicts cognitive control and intelligence. *J Neurosci*. 32:8988-8999.
9. Driesen NR, McCarthy G, Bhagwagar Z, Bloch M, Calhoun V, D'Souza DC, et al. (2013): Relationship of resting brain hyperconnectivity and schizophrenia-like symptoms produced by the NMDA receptor antagonist ketamine in humans. *Mol Psychiatry*. 18:1199-1204.
10. Driesen NR, McCarthy G, Bhagwagar Z, Bloch MH, Calhoun VD, D'Souza DC, et al. (2013): The impact of NMDA receptor blockade on human working memory-related prefrontal function and connectivity. *Neuropsychopharmacology*. 38:2613-2622.
11. Power JD, Barnes KA, Snyder AZ, Schlaggar BL, Petersen SE (2012): Spurious but systematic correlations in functional connectivity MRI networks arise from subject motion. *Neuroimage*. 59:2142-2154.
12. Liang X, Zou Q, He Y, Yang Y (2013): Coupling of functional connectivity and regional cerebral blood flow reveals a physiological basis for network hubs of the human brain. *Proc Natl Acad Sci U S A*. 110:1929-1934.
13. Cole MW, Pathak S, Schneider W (2010): Identifying the brain's most globally connected regions. *NeuroImage*. 49:3132-3148.
14. Fischl B (2012): FreeSurfer. *Neuroimage*. 62:774-781.
15. Abdallah CG, Coplan JD, Jackowski A, Sato JR, Mao X, Shungu DC, et al. (2012): Riluzole effect on occipital cortex: a structural and spectroscopy pilot study. *Neurosci Lett*. 530:103-107.
16. Abdallah CG, Coplan JD, Jackowski A, Sato JR, Mao X, Shungu DC, et al. (2013): A pilot study of hippocampal volume and N-acetylaspartate (NAA) as response biomarkers in riluzole-treated patients with GAD. *Eur Neuropsychopharmacol*. 23:276-284.

17. Yeo BT, Krienen FM, Sepulcre J, Sabuncu MR, Lashkari D, Hollinshead M, et al. (2011): The organization of the human cerebral cortex estimated by intrinsic functional connectivity. *J Neurophysiol*. 106:1125-1165.
18. Cole MW, Bassett DS, Power JD, Braver TS, Petersen SE (2014): Intrinsic and task-evoked network architectures of the human brain. *Neuron*. 83:238-251.
19. Cole MW, Yang GJ, Murray JD, Repovs G, Anticevic A (2016): Functional connectivity change as shared signal dynamics. *J Neurosci Methods*. 259:22-39.
20. Winkler AM, Ridgway GR, Webster MA, Smith SM, Nichols TE (2014): Permutation inference for the general linear model. *Neuroimage*. 92:381-397.